Radiology

REVIEWS AND COMMENTARY • SPECIAL REPORT

The QIBA Profile for Diffusion-Weighted MRI: Apparent Diffusion Coefficient as a Quantitative Imaging Biomarker

Michael A. Boss, PhD • Dariya Malyarenko, PhD • Savannah Partridge, PhD • Nancy Obuchowski, PhD • Amita Shukla-Dave, PhD • Jessica M. Winfield, PhD • Clifton D. Fuller, MD, PhD • Kevin Miller, MBA • Virendra Mishra, PhD • Michael Ohliger, MD, PhD • Lisa J. Wilmes, PhD • Raj Attariwala, MD, PhD • Trevor Andrews, PhD • Nandita M. deSouza, MD • Daniel J. Margolis, MD • Thomas L. Chenevert, PhD

From the Center for Research and Innovation, American College of Radiology, 50 S 16th St, Philadelphia, PA 19102 (M.A.B.); Department of Radiology, University of Michigan, Ann Arbor, Mich (D.M., T.L.C.); Department of Radiology, University of Washington, Seattle, Wash (S.P.); Department of Quantitative Health Sciences, Cleveland Clinic, Cleveland, Ohio (N.O.); Departments of Medical Physics and Radiology, Memorial Sloan Kettering Cancer Center, New York, NY (A.S.D.); The Institute of Cancer Research, London, UK (J.M.W., N.M.d.S.); The Royal Marsden NHS Foundation Trust, London, UK (J.M.W., N.M.d.S.); Department of Radiation Oncology, The University of Texas MD Anderson Cancer Center, Houston, Tex (C.D.F.); CaliberMRI, Boulder, Colo (K.M.); Department of Radiology, University of Alabama at Birmingham, Birmingham, Ala (V.M.); Department of Radiology and Biomedical Imaging, University of California, San Francisco, San Francisco, Calif (M.O., L.J.W.); Aim Medical Imaging, Vancouver, Canada (R.A.); Mallinckrodt Institute of Radiology, Washington University School of Medicine, St Louis, Mo (T.A.); and Department of Radiology, Weill Cornell Medical College, New York, NY (D.J.M.). Received November 15, 2023; revision requested January 24, 2024; revision received February 23; accepted March 21. **Address correspondence to** M.A.B. (email: *michael.a.boss@gmail.com*).

This work has been supported in part with federal funds from the National Institute of Biomedical Imaging and Bioengineering, National Institutes of Health, and U.S. Department of Health and Human Services under contract no. HHSN268201000050C; National Cancer Institute grant no. R01 CA190299, R01 CA207290, R01 CA248192, U01 CA140204, U01 CA225427, and U24 CA237683; and National Institute of Neurological Disorders and Stroke grant no. R01 NS117547. This study represents independent research funded by the National Institute for Health and Care Research (NIHR) Biomedical Research Centre at The Royal Marsden NHS Foundation Trust and The Institute of Cancer Research, London, and by the Royal Marsden Cancer Charity. The views expressed are those of the authors and not necessarily those of the NIHR or the Department of Health and Social Care.

Conflicts of interest are listed at the end of this article.

See also the editorial by Haider in this issue.

Radiology 2024; 313(1):e233055 • https://doi.org/10.1148/radiol.233055 • Content codes: BQ MR

The apparent diffusion coefficient (ADC) provides a quantitative measure of water mobility that can be used to probe alterations in tissue microstructure due to disease or treatment. Establishment of the accepted level of variance in ADC measurements for each clinical application is critical for its successful implementation. The Diffusion-Weighted Imaging Biomarker Committee of the Quantitative Imaging Biomarkers Alliance (QIBA) has recently advanced the ADC Profile from the consensus to clinically feasible stage for the brain, liver, prostate, and breast. This profile distills multiple studies on ADC repeatability and describes detailed procedures to achieve stated performance claims on an observed ADC change within acceptable confidence limits. In addition to reviewing the current ADC Profile claims, this report has used recent literature to develop proposed updates for establishing metrology benchmarks for mean lesion ADC change that account for measurement variance. Specifically, changes in mean ADC exceeding 8% for brain lesions, 27% for liver lesions, 27% for prostate lesions, and 15% for breast lesions are claimed to represent true changes with 95% confidence. This report also discusses the development of the ADC Profile, highlighting its various stages, and describes the workflow essential to achieving a standardized implementation of advanced quantitative diffusion-weighted MRI in the clinic. The presented QIBA ADC Profile guidelines should enable successful clinical application of ADC as a quantitative imaging biomarker and ensure reproducible ADC measurements that can be used to confidently evaluate longitudinal changes and treatment response for individual patients.

Supplemental material is available for this article.

The apparent diffusion coefficient (ADC) derived from MRI with diffusion-weighted imaging (DWI) provides a quantitative measure of water mobility, which can be used to assess alterations in the tissue microenvironment due to disease (1,2) or treatment (3,4). ADC maps are used in a variety of pathologic abnormalities to improve disease detection and characterization. For example, lower ADC values may indicate higher tissue cellularity correlated with the pathologic grade in prostate cancer (2). ADC-aided grading of prostate lesions could spare biopsy when assessing progression in patients managed with active surveillance (5). In a multicenter trial of breast cancer, the change in ADC across time points has been shown to predict pathologic complete response to neoadjuvant chemotherapy (3), while in phase II trials in patients with glioblastoma, ADC has been promising for predicting the survival benefit of targeted therapies (6). ADC has also been shown to aid response assessment for patients with hepatocellular carcinoma (4). However, a lack of measurement standardization and insufficient knowledge of the acceptable level of variance impede the full exploitation of ADC as a quantitative imaging metric.

Standardizing quantitative imaging biomarkers for clinical trials and practice has been the goal of the Quantitative Imaging Biomarker Alliance (QIBA) since its creation by the RSNA in 2007. The DWI Biomarker Committee of QIBA has undertaken this work for ADC. As with any quantitative measure, proper interpretation of ADC numeric values requires established CIs to define the thresholds for consequential change relative to measurement error. The confidence of ADC measurements for different organ types is determined by a combination of accuracy (ie, bias, the difference between measured value and "truth") and precision (ie, repeatability, proportional to the within-subject coefficient of variation [wCV]), holding experimental conditions constant (7,8). The DWI Biomarker Committee's work in this area culminated in the current QIBA ADC Profile (9). The profile document reports technical performance claims for ADC achieved by conforming to specifications for the main elements of the quantitative DWI measurement workflow. These specifications define the limits for essential image acquisition and processing parameters to achieve the claimed ADC precision.

Abbreviations

ADC = apparent diffusion coefficient, DRO = digital reference object, DWI = diffusion-weighted imaging, QIBA = Quantitative Imaging Biomarker Alliance, ROI = region of interest, wCV = within-subject coefficient of variation, wSD = within-subject SD

Summary

The claims and procedures of the Quantitative Imaging Biomarker Alliance Diffusion-Weighted Imaging Biomarker Committee are summarized for apparent diffusion coefficient as a quantitative biomarker to monitor lesions in the brain, liver, prostate, and breast.

Essentials

- For lesions measured on clinical scanners with standard diffusion-weighted single-shot echo-planar imaging, a measured change in the apparent diffusion coefficient exceeding 8% in brain, 27% in liver, 27% in prostate, and 15% in breast can be considered to represent a true change with 95% confidence.
- These claims hold when the same MRI scanner and protocol is used for longitudinal measurements or when the technical bias between different scan protocols is minimized.
- CIs for quantitative diffusion metrics derived from new advanced scan protocols (eg, artificial intelligence) must be established using test-retest studies in at least 35 individuals with repositioning and characterization of bias and linearity using phantoms with calibrated values.

This special report describes the QIBA process to establish CIs for reliable detection of ADC change exceeding measurement error; reviews the current ADC precision claims for liver, brain, breast, and prostate of the ADC Profile; and proposes updated claims based on recent studies published after the consensus revision of the ADC Profile. The report also provides general guidelines for generating future precision claims, which can be used for new quantitative DWI acquisition methods and advanced models for tissue diffusion parameters beyond monoexponential, single-compartment ADC.

ADC Profile Development, Considerations, and Evaluations

Profile Stages

Originally, the QIBA DWI Biomarker Committee examined the peer-reviewed literature to identify studies containing ADC repeatability data with adequate description of methods and statistics. Following established QIBA processes, the initial form and content of the QIBA ADC Profile was open for public comment (stage 1), receiving input from experts, professional organizations, and other stakeholders, including industry. Resolution of public comments led to a consensus document (stage 2) published in 2019. The QIBA DWI Biomarker Committee undertook several groundwork projects to supplement key missing elements for profile conformance testing, including development of a physical phantom, quality control analysis software, and an ADC signal-to-noise ratio digital reference object (DRO). After implementation at four independent clinical sites that applied technical conformance procedures and evaluated overall clarity and feasibility of the process (10,11), the current ADC Profile advanced to the clinically feasible stage (stage 3) in 2022 (9).

ADC Accuracy and Precision Evaluation

The quantitative ADC metric is derived from two or more DWI acquisitions assuming monoexponential dependence of DWI intensity on b value: $S(b) = S_0 e^{-b \cdot ADC}$. Nonmonoexponential tissue models to address mixed diffusion compartments were beyond the scope of the current ADC Profile. Key contributors to systematic technical ADC bias include dependencies on acquisition protocol and MRI system hardware design (12). Absolute accuracy measurement requires ground truth diffusion coefficient values and is typically assessed using physical phantoms containing precisely known diffusion media (10,12,13) and enhanced using standardized acquisition protocols (3,14,15).

Precision of tissue ADC measurements was derived from test-retest (ie, scan-rescan with repositioning) repeatability studies with controllable factors contributing to measurement variability held constant (7,11). Importantly, the intraclass correlation coefficient, which is often reported in the literature, was not considered when developing the ADC Profile, as it is not appropriate for establishing or validating ADC precision. Furthermore, in vivo repeatability assessment should be performed with human patients and protocols on multiple platforms, as phantom studies do not reflect all relevant sources of variability (11,14,16).

The within-subject SD (wSD) characterizes measurement repeatability (7,11). When wSD positively correlates with ADC, the wCV and scaled percent repeatability coefficient (equal to $2.77 \cdot \text{wCV} \cdot 100\%$) are independent of the magnitude of ADC and are appropriate measures of precision. Otherwise, wSD (and repeatability coefficient) in ADC units should be used. To ensure sufficient sample size for nominal 95% CIs of the derived repeatability coefficients, multicenter studies with at least 35 patients (17) were recommended to form precision claims in the ADC Profile. When aggregate wCV was derived from several (small) single-center studies, it was computed using reported sample size for each study as a weighting factor. Here, wCV_i is the wCV from the i^{th} article of n total articles, and N_j is the sample size from the i^{th} study (18):

$$wCV = \sqrt{\left(\sum_{j=1}^{n} wCV_j^2 \times N_j\right) / \left(\sum_{j=1}^{n} N_j\right)}.$$

Organ-Specific Approach

ADC varies across disease sites, and each disease site presents unique diffusion imaging challenges; thus, the observed wCV and the associated DWI protocols differ across organs. For example, while the brain is relatively immobile, air in the sinuses can introduce susceptibility-induced artifacts; bulk motion in the liver (respiratory and cardiac pulsation) can adversely affect the determination of ADC. For this reason, the current QIBA ADC Profile provides claims on the basis of disease site, focusing on the brain, liver, prostate, and breast. At the time of ADC Profile writing, other organs were excluded due to lack of sufficient published test-retest data to support a claim statement.

Current ADC Profile Claims and Proposed Updates

ADC Profile claims establish repeatability coefficient (7,11) thresholds, which can be used to determine whether a

measured change in mean ADC values of lesions reliably represents a true change. If the measured change in ADC exceeds the repeatability coefficient threshold reported for each organ type (Table 1), it indicates that a true change has occurred with 95% confidence. A 95% CI for the true change in ADC of a lesion is given below, based on wCV, where Y_1 and Y_2 are the ADC measurements at the two time points:

$$(Y_2 - Y_1) \pm 1.96 \times \sqrt{(Y_1 \times \text{wCV})^2 + (Y_2 \times \text{wCV})^2}.$$

Note that this corresponds to a specificity of 95%, since sensitivity to detect true change cannot be estimated from test-retest studies assuming unchanged biologic condition. Table 1 (left columns) lists the current stage 3 ADC Profile claims, with repeatability coefficients provided for the four organ systems.

The claims in the current profile (9) derive from a review of published test-retest studies before 2019 (when the profile was first published as a stage 2 consensus document). The derived repeatability threshold for breast is based on results from a single multicenter study (15) with sufficiently large sample size (ie, 71 patients). For other organs, where individual study groups were small but image and analysis protocol parameters were reasonably similar across studies, claims were derived from a meta-analysis of combined single-center studies with pooled sample size greater than 35 patients (17) (eg, prostate [19–21]). The available literature included both healthy tissue and lesions for prostate, brain (22–24), and liver (25–27), but only lesions in breast.

The preparation of this report resulted in a review of the recent test-retest ADC literature to identify any studies that could further inform and refine the claims for included organs. These studies allowed claim derivation exclusively for lesions in all four organs. Table 1 (right columns) shows the proposed updates informed by this literature, particularly for prostate (14,28–30), while also excluding studies with healthy volunteers for brain (6,24) and liver (25,26). The resulting updated repeatability thresholds for lesion ADC notably reduce CIs for prostate (from 47% to 27%) and marginally for brain (from 11% to 8%) while slightly increasing them for liver (from 26% to 27%) and breast (from 13% to 15%). Of note is that both current and updated profile claims (Table 1) enable only longitudinal ADC comparison for individual patients; profile document updates are forthcoming.

Conditions for the ADC Profile Claims to Be Valid

The claimed repeatability thresholds only hold if DWI acquisition and processing parameters conform to profile specifications (9) summarized in this section and comply with the acceptable acquisition and processing protocol parameters, detailed in specification tables included in Appendix S1 of this report. The profile claims represent the current benchmark for ADC precision for a distinct protocol workflow

Table 1: Current QIBA Profile for Apparent Diffusion Coefficient Claim Statements and Proposed Updates to Claim Statements Reflecting the Latest Test-Retest Literature in Four Organs

	Current Profile Claims				Proposed Updates to Claims			
Organ	References	ROI Size Range (cm^3)	wCV	Repeatability Coefficient (%)*	References	ROI Size Range (cm^3)	wCV	Repeatability Coefficient (%)*
Brain	Pfefferbaum et al, 2003 (22); Bonekamp et al, 2007 (23); Paldino et al, 2009 (24)	Not reported	0.04	11	Paldino et al, 2009 (24); Ellingson et al, 2017 (6)†	Not reported	0.026	8
Liver	Miquel et al, 2012 (27); Heijmen et al, 2013 (26); Deckers et al, 2014 (25)	0.7–130.4	0.094	26	Heijmen et al, 2013 (26); Deckers et al, 2014 (25)†	0.7–130.4	0.095	27
Prostate	Gibbs et al, 2007 (20); Litjens et al, 2012 (21); Fedorov et al, 2017 (19)	1.2–3.2‡	0.17	47	Boss et al, 2022 (14); Barrett et al, 2019 (30); Zhang et al, 2023 (28); Rogers et al, 2023 (29)	0.2–1.3	0.097	27
Breast	Newitt et al, 2018 (15)	0.2–20	0.047	13	Newitt et al, 2020 (16)§	0.2–20	0.054	15

Note.—QIBA = Quantitative Imaging Biomarker Alliance, ROI = region of interest, wCV = within-subject coefficient of variation.

* Calculated using the following equation: repeatability coefficient percent = 2.77 × wCV × 100%.

† While the original cited literature included mixed healthy tissue and lesion data for brain, liver, and prostate, the updated publications provide lesion-specific test-retest metrics.

‡ Single section.

§ In the study by Newitt et al (16), wCV calculation was corrected as $wCV = \sqrt{\text{MEAN}\left(\text{variance} / \text{mean}^2\right)}$ from the earlier study by Newitt et al (15) ($wCV = \sqrt{\text{MEAN}(\text{variance})} / \text{mean}$), where (variance/mean^2) is the variance of replicate measurements for each patient divided by the squared mean of the measurements for that patient, and MEAN is the average over the n patients.

with single-shot echo-planar DWI readout. The current claims are valid at both 1.5 and 3.0 T, excepting prostate, which is only informed by data at 3.0 T. The same scanner and protocol are used for intrapatient test-retest scans to assess precision metrics and inform the claims.

The current ADC Profile claims assume that wCV is constant for tissue regions in the specified size (independent of imaging time), the signal-to-noise ratio of the tissue region on the $b = 0$ image is at least 50, and the measured ADC is linear (slope ≈ 1) with respect to the true ADC value over the tissue-specific range of 0.3×10^{-3} mm^2/sec to 3.0×10^{-3} mm^2/sec. Common practice is to avoid image artifacts and exclude voxels with nonphysical water diffusion values (ADC <0 or ADC >3.0×10^{-3} mm^2/sec for 37 °C body temperature) in mean ADC calculation (31). The repeatability literature used to inform the claims generally excludes poor-quality and protocol-deviating examinations (14,15); the profile requires sufficient image quality and protocol adherence to be valid.

The claims are defined for mean ADC values within the region of interest (ROI) delineated by one reader for test and retest scans independently. The typical ADC ROI sizes reported by references are listed in Table 1 of this report. The ADC Profile illustrates common DWI artifacts leading to unreliable ADC values. It provides guidelines to avoid artifacts in ROI selection and mitigate bias (sections 3.10, 3.11, and 3.13 in reference 9), as well as organ-specific details of required image processing and quality control steps (9).

Longitudinal and Cross-Sectional ADC Applications

The repeatability coefficient thresholds provided in the profile claims can be used to establish CIs to evaluate changes in ADC values related to therapy response over time ("longitudinal" or serial measurements) of individual patients (32). For example, if the observed change in ADC of a lesion for an individual patient exceeds 15% following treatment, it can be considered a true change with 95% confidence for brain and breast lesions, but not for prostate and liver (Table 1). Beyond constant wCV with time, longitudinal applications require that measurement bias be the same for both imaging points, canceling out systematic offset between longitudinal ADC measurements. Thus, patients should be scanned on the same MRI system with a fixed protocol for all imaging points during longitudinal study (3,4,6,14).

Quantitative ADC thresholds for "cross-sectional" comparison (eg, between groups with and without disease) may be used for cancer detection, grading, and staging in prostate and breast. This type of diagnostic evaluation needs to assess measurement bias and repeatability. Base-level MRI system technical bias can be measured when the true ADC value is known, which is possible using physical phantoms (11–13) but usually is not feasible for patients. Another way to use precision as a 95% CI for cross-sectional comparisons is to ensure negligible measurement bias (eg, by protocol standardization) (14,15). When negligible bias exists, the cross-sectional claim can be compiled based solely on precision, where the difference between two ADC measurements ($Y_2 - Y_1$) is replaced by the difference between the "disease" and "control" ADCs, accounting for their respective wCVs.

The recent literature in healthy volunteers, using acquisition protocols largely aligning with the requirements of the ADC Profile for each included organ, suggests that organ-specific differences in repeatability for normal versus malignant lesion ADC may be substantial (Table 2) and need to be accounted for. For example, malignant lesion wCV of 9.7% (Table 1) (14,28–30) is higher than wCV of 6.1% (33,34) for normal prostate peripheral zone. On the other hand, wCV of 9.4% reported for benign breast lesions (35) is higher than that of the malignant lesions (wCV of 5.4%) (16). Assuming minimal bias, these data suggest that cross-sectional application of ADC in the peripheral zone of the prostate could be based on a wCV of 0.061 in normal tissue (33,34) and of 0.097 in the diseased tissue.

ADC Profile Implementation Workflow

The QIBA ADC Profile provides a structured roadmap for imaging centers, scanner manufacturers, radiologists, and other stakeholders that seek use of quantitative ADC readouts for disease characterization and/or monitoring response to treatment (Figure). As detailed in the profile, multiple elements must function in concert to achieve the claims. The DWI Biomarker Committee has created checklists for each element *(https://qibawiki.rsna.org/index.php/QIBA_Profile_Conformance)*. Site personnel can complete these checklists to serve as an attestation of full or partial profile conformance. To implement the profile, it is recommended that users define the relevant key participants in the ADC workflow (Figure) and use the checklists to confirm conformance to their specifications.

Actors, Activities, and Checklists

The profile organizes materials in sections that describe necessary elements ("actors") in the ADC workflow, along with specifications for each element to meet the performance claims. The ADC Profile elements that influence performance for clinical implementation are site, acquisition device, scanner operator, image analyst, reconstruction software, and image analysis tool. The purpose of activities is to ensure that ADC measurements achieve the precision stated in the profile claims. In effect, the checklists summarize requirements (specifications) to meet the claims. Some of the specifications are general (eg, DWI phantoms), while others are organ-specific.

Quality Assurance and Conformance Testing

Technical conformance testing of the MRI scanner is the essential first step (Figure) to accurate ADC measurements, since its performance can be objectively assessed using physical DWI phantoms and standardized test procedures. Toward this end, the ADC Profile provides guidelines to benchmark DWI acquisition performance and measure ADC bias with detailed description of four essential elements: *(a)* suitable DWI phantom(s), *(b)* DWI scan protocols, *(c)* target performance specifications, and *(d)* analysis software to assess performance derived from DWI Digital Imaging and Communications in Medicine, or DICOM, headers.

The profile provides details of the scanner assessment procedures and corresponding specifications (9). Updating

Table 2: Summary of Recent Repeatability Studies in Controls Without Malignancy That Are Not Included in the Current QIBA Profile for Apparent Diffusion Coefficient

Organ	Reference	wCV (%)	Tissue	ROI or VOI Size	No. of Scanners	Field Strength (T)	*b* Values (sec/mm^2)	No. of Individuals	Test-Retest Schedule
Brain	Michoux et al, 2021 (34)*	3.1	Normal WM	2.49 cm^2	3	3.0	0, 150, 1000	24 (8 per system)	1 hour and 1–7 days
Liver	Michoux et al, 2021 (34)	8	Left liver lobe	4.1 cm^2	3	3.0	0, 150, 1000	24 (8 per system)	1 hour and 1–7 days
Prostate†									
	Rogers et al, 2023 (29)	9	nTZ	1.7–13.6 cm^2	1	3.0	0, 1500	7	Repositioned
	Hoang-Dinh et al, 2022 (33)	6	Whole nPZ	1 midgland section	2	1.5	Multiple, 0–800	49	Morning and evening
	Michoux et al, 2021 (34)*	5. 16.2	nCZ nPZ	1.65 cm^2 1.84 cm^2	3	3.0	0, 150, 1000	24 (8 per system)	1 hour and 1–7 days
Breast									
	Jerome et al, 2021 (35)	9.4	Benign lesion	0.3–25.4 cm^3 VOI coefficient of variation = 13.9%	1	3.0	Multiple, 0–700	20 (26 samples)	2–10 days
	Sorace et al, 2018 (38)	3.7	Normal FG	Whole single breast FG VOI	1	3.0	0, 200, 800	10	Same day

Note.—FG = fibroglandular, nCZ = normal central zone, nPZ = normal peripheral zone, nTZ = normal transition zone, QIBA = Quantitative Imaging Biomarker Alliance, ROI = region of interest, VOI = volume of interest, wCV = within-subject coefficient of variation, WM = white matter.

* The study by Michoux et al (34) used 6-mm sections, which is slightly larger than acceptable for brain and prostate, due to a whole-body diffusion-weighted imaging protocol.

† Zone-dependent repeatability observed for prostate.

profile claims based on purportedly improved DWI technology (eg, hardware, acquisition, or data processing protocol) requires a test-retest study in at least 35 individuals and wSD dependence on mean ADC assessed to use either the repeatability coefficient (derived from wSD) or percent repeatability coefficient (derived from wCV).

Physical and Digital Reference Objects for ADC Bias Assessment

The QIBA ADC Profile describes physical phantoms and DROs, with calibrated or controlled ADC to assess bias. Physical phantoms help assess system bias, potentially correct it (12,13), and ensure that measured ADC scales linearly with true ADC over the range of interest (ideally, with slope of 1). Characterization of linearity is particularly important in the context of enabling tissue classification based on a single quantitative measurement. Given the lack of absolute truth in tissue ADC values, QIBA recommends assessment of MRI system linearity with use of physical phantoms containing an array of known diffusivity values, such as polyvinylpyrrolidone-based phantoms (13,36).

For assessment of ADC spatial uniformity over the imaged field of view or at offsets relevant to off-center anatomy (eg, breast, liver), single-value uniform ADC phantoms are useful (11,12). Since diffusion is thermally driven, internal phantom temperature needs to be controlled (eg, with an ice water bath) (12,13) or have built-in precise temperature readout for calibrated determination of true values (36,37). Commercial phantoms (eg, CaliberMRI [10]) are user-friendly in the clinical environment and have the benefit of temperature calibration and sustainable materials. Home-built ice water–based phantoms (11,12) are economical and offer absolute temperature control, but preparation is more cumbersome, and images are distorted due to susceptibility artifacts.

DROs can be used to detect bias introduced by the algorithm used to convert DWI to ADC maps. Digital phantoms are built by forward modeling of the DWI signal and offer low-cost alternatives to the assessment of the ADC map generation software. However, the input DRO parameters should include relevant ranges of *b* values and a realistic noise model to mimic conditions observed for tissue DWI acquisition. Linearity of ADC map generation routines (from DWI) may also be assessed with use of realistic DROs.

ADC Profile Limitations and Gaps in Knowledge

Need for More Organ-Specific Test-Retest and Interreader Data

For future incorporation of additional organ systems and clinical conditions, new studies need to report Bland-Altman statistics, including estimates and 95% CIs for wSD or wCV, not just intraclass correlation coefficients or Dice similarity coefficients. To assess realistic variability for longitudinal studies, patients should be repositioned between test and retest scan acquisitions. These studies must provide

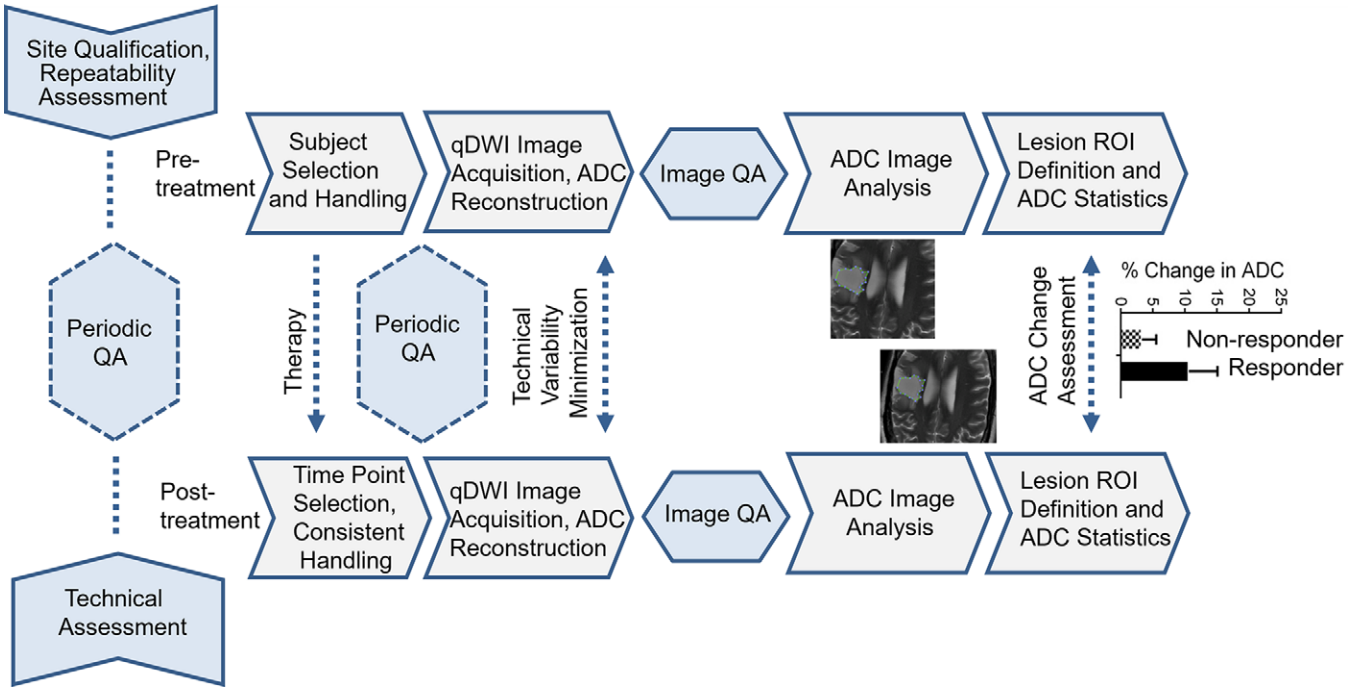

Diagram shows typical quantitative diffusion-weighted imaging (qDWI) trial workflow with key Quantitative Imaging Biomarker Alliance apparent diffusion coefficient (ADC) profile activities. The required workflow components are shown in the arrow-shaped boxes, with activity guidelines detailed in the Specification Tables (9) and Profile Checklist (available at *https://qibawiki.rsna.org/index.php/QIBA_Profile_Conformance*). Initial site qualification and periodic quality assurance (QA) between imaging time points, as well as persistent image quality assurance (blue shapes), are essential to ensure consistent image acquisition and processing protocols for achievement of the claimed ADC precision and defining thresholds for therapy response assessment of individual patients (as illustrated for a brain lesion). ROI = region of interest.

a sample size of at least 35 patients or be based on combined meta-analysis and account for interlesion correlations (in the case of multiple lesions per patient) by reporting an effective sample size (18,28). Such meta-analysis presents a challenge when individual studies have inconsistent protocols (35,38) or report insufficient details, such as multiple lesion correlation (25,26), which may inadvertently bias derived thresholds of change. An additional challenge of test-retest DWI studies is acquiring sufficient sample size and high-quality data for analysis; for example, two separate DWI repeatability studies in breast and prostate had to exclude approximately 17% of examinations due to issues of image quality or protocol deviation (3,14).

Furthermore, current profile claims do not account for interreader variability. Higher variability is expected for multiple readers, such as two readers for longitudinal scans with interreader wCV_i, when the resulting $wCV = \sqrt{wCV_i^2 + wCV_0^2}$, where wCV_0 is the single-reader test-retest coefficient of variation (Table 1). The studies of interreader variability report wCV_i within the order of or exceeding the test-retest precision for breast (4.5%–6% vs 4.6%–6.5%) (15,39) and better than test-retest precision for prostate (2%–5% vs 6%–10.6%) (14,28,40).

Gaps in Cross-Sectional Applications

Current ADC Profile claims provide thresholds for longitudinal changes but do not enable general cross-sectional application with arbitrary bias. Small sample sizes with unharmonized acquisition protocols and single-center studies inform the majority of the normal-tissue ADC repeatability literature (Table 2), impeding cross-sectional claim formulation for all organs. The deviation of tissue diffusion parameters from the assumption of monoexponential behavior typically results in ADC biases, dependent on the *b* value range and degree of suppression of the non–tissue-of-interest signal (eg, from fat in breast or bone marrow). Current physical ADC phantoms usually have high signal-to-noise ratio and do not match other tissue parameters (like relaxivity or multicompartment diffusion) and therefore provide a best-case assessment of protocol repeatability. Ideally, a multiparametric phantom with realistic ADC ranges and relaxation parameters is needed for bias evaluation with *b* values and signal-to-noise ratio used by the in vivo organ-specific DWI protocol. Bias assessment should also include realistic filtering of nonphysical ADC values. Importantly, additional studies are needed to evaluate ADC sensitivity for target clinical applications, since reported repeatability thresholds (based on test-retest studies) only determine specificity, as these studies are necessarily based on no-change biologic conditions. The desired cross-sectional comparisons will also require information on ADC ranges for specific clinical conditions (eg, indolent vs aggressive prostate cancer).

Reporting of ROI Size and Delineation

The current repeatability literature often lacks consistent ROI information, making the systematic study of how ROI size impacts the calculation of repeatability coefficients challenging. ROI delineation is anticipated to be a large contributor to the observed variability in measured ADC. This effect varies by organ due to factors such as minimum size and approach to ROI delineation of organs and/or lesions (eg, type of contrast material used, manual vs automated

segmentation). Several studies indicate that repeatability coefficients depend on ROI size and are specifically related to the number of voxels included in the ROI (approximately $1/\sqrt{N}$) (14,15,28,29). For prostate ADC, better precision (lower repeatability coefficients) has been reported for larger ROIs in whole prostate (14) and whole normal peripheral zone (33) (repeatability coefficient, 10% and 11%, respectively) versus peripheral zone lesion (repeatability coefficient, 27% [Table 1]). Reduced wCVs were noted for three-dimensional volume versus single-section two-dimensional ROI analysis for both breast (15) and prostate (28).

Several recent studies evaluated interreader agreement for the ROIs and found repeatability coefficients of 10%–14% for prostate lesions (14,28,40) and 17%–22% for breast lesions (15,39,41). These investigations suggest that a sizable contributor to decreased repeatability is the imprecision of manual lesion segmentation. While scan protocol optimization can improve ADC measurement precision, standardization of segmentation and its automation together with better image registration to high-spatial-resolution reference images could help reduce interreader discrepancy. Recent consensus recommendations have described standardization criteria for lesion segmentation (42), which will aid the adoption of standardized methods and consistent reporting of ROIs. A detailed description of ROI delineation should be required for publication of future test-retest studies, which will better inform future versions of the ADC Profile.

New ADC Developments and Conclusions

Leveraging the ADC Profile in an ever-evolving landscape of new and improved DWI methods, advanced quantitative models, and clinical protocols can result in more consistent ADC evaluations across patients, sites, and time. The profile is a dynamic document, informed by the current literature and even updated by it: there has been a nearly twofold improvement of precision for prostate ADC compared with studies before 2019 (Table 1). The current claims should be viewed as baseline performance guidelines achievable when the described protocols are standardized and imaging parameter values meet the acceptable criteria or better (Appendix S1). Adjustments to existing claims are possible as additional studies providing appropriate data become available (11,28).

When protocol improvements are desired, the bias across systems needs to be assessed with well-characterized phantoms, and either minimized by standardization or measured and accounted for in ADC CIs. Test-retest repeatability studies with a sufficient sample size must also be conducted to establish repeatability coefficients and compared with benchmark values when available. For example, a recent study by Zhang et al (28) for prostate ADC indicated consistent repeatability coefficients of 22% for a readout-segmented echo-planar imaging protocol versus single-shot echo-planar DWI using three-dimensional volume ROI. However, this study reported a substantial decline in repeatability for a single-section two-dimensional ROI between readout-segmented and single-shot echo-planar imaging (47% vs 25%). New DWI protocols including multishot, reduced field of view, and reverse-polarity gradients require bias testing with respect to standard echo-planar imaging (used in current claims) but are expected to reduce artifact and improve repeatability.

As clinical need drives the utility of ADC, the profile could be expanded when sufficient repeatability studies are performed for new clinical applications. For example, quantitative ADC may be applied for radiation dose optimization in head and neck cancer trials. Evaluation of the repeatability of this metric in a small pilot study of nine patients showed promising results (repeatability coefficient, 3%–9%) (43). Additional multisite test-retest studies in at least 26 individuals with similar acquisition protocols would be needed to achieve the minimum pooled sample size of 35 to formulate the precision claim for this application. Notably, the recent development of hybrid MRI–linear accelerator devices has entailed assessment of ADC repeatability on novel imaging systems with differing technical provisions, coil platforms, and field strengths across multiple organ sites, with application in the brain achieving an ADC repeatability coefficient of 5% with 95% confidence (44), free-breathing imaging of the liver achieving a repeatability coefficient of 43% (45), and head and neck tumors achieving a mean repeatability coefficient of 30% (46,47). Interpretation of the clinical relevance of any observed changes should consider individual circumstances and anticipated pathologic variations.

Other approaches are exploring new DWI-based biomarkers beyond ADC to assess clinical or biologic change. For instance, intravoxel incoherent motion, restriction spectrum imaging, and diffusion kurtosis model metrics may have higher sensitivity for specific disease changes compared with ADC (43). Their corresponding acquisition protocols need evaluation accordingly for bias and precision. Other metrics for ROI histograms, beyond the mean ADC values, may also be tested (16). However, these are often expected to have increasing variability with decreasing ROI size (29,41) and thus would be clinically useful only when their corresponding effect exceeds the mean ADC changes.

Few quantitative biomarkers in imaging are as versatile and robust as apparent diffusion coefficient (8,11). Its simplicity of acquisition, ease of implementation, and widespread availability mean that it is ripe for clinical exploitation (1,3,6,14), particularly in an era of automation and machine learning in radiology (48,49). Standardization and harmonization will expand its use in this setting (1,8,11), improving diagnostic accuracy and response assessment for individual patients and their personalized treatments.

Deputy Editor: Vicky Goh
Scientific Editor: Ariane Panzer

Acknowledgments: The authors give their many thanks to the RSNA staff who have tirelessly supported this profile's development: Joe Koudelik; Susan Stanfa, MLIS; Julie Lisiecki, MEd; and Fiona Miller. Our efforts in QIBA have been guided and encouraged by Alex Guimaraes, MD, PhD; Gudrun Zahlmann, PhD; Mark Rosen, MD, PhD; and notably, Edward F. Jackson, PhD.

Author contributions: Guarantors of integrity of entire study, **M.A.B., D.M., T.L.C.**; study concepts/study design or data acquisition or data analysis/interpretation, all authors; manuscript drafting or manuscript revision for important intellectual content, all authors; approval of final version of submitted manuscript, all authors; agrees to ensure any questions related to the work are appropriately resolved, all authors; literature research, **M.A.B., D.M., S.P., A.S.D., J.M.W., C.D.F., V.M., L.J.W., R.A., D.J.M., T.L.C.**; clinical studies, **M.A.B., R.A.**; experimental studies, **M.A.B., L.J.W., R.A., T.L.C.**; statistical analysis, **M.A.B., D.M., N.O., C.D.F.**; and manuscript editing,

M.A.B., D.M., S.P., N.O., A.S.D., J.M.W., C.D.F., K.M., V.M., M.O., R.A., T.A., N.M.d.S., D.J.M., T.L.C.

Disclosures of conflicts of interest: **M.A.B.** Co-chair of the DWI Biomarker Committee, co-chair of the MR Coordinating Committee, and vice-chair of the Process Committee for the RSNA Quantitative Imaging Biomarkers Alliance (QIBA). **D.M.** Subcontract grant to institution from the National Institute of Biomedical Imaging and Bioengineering (NIBIB) and grants from the National Institutes of Health (NIH); co-chair of the DWI Biomarker Committee for QIBA. **S.P.** Grants to institution from the NIH and National Cancer Institute (NCI); chair of the NCI Quantitative Imaging Network Executive Committee (unpaid); in-kind research support to institution from Philips Healthcare. **N.O.** Statistical support to institution from RSNA; statistical support contracts with institution and NIH, Siemens, QURE, Takeda, and Foundation for the NIH; royalties from Wiley & Sons; honoraria from the RSNA; participation on a data safety monitoring board for Eastern Cooperative Oncology Group–American College of Radiology Imaging Network; member of the NCI Clinical Imaging Steering Committee; patent pending for automated identification of vascular pathology in CT images; member of the RSNA Quantitative Imaging Committee (unpaid). **A.S.D.** No relevant relationships. **J.M.W.** No relevant relationships. **C.D.F.** Grants to institution from NIH, National Institute of Dental and Craniofacial Research, NCI, NIBIB, National Science Foundation Division of Civil, Mechanical, and Manufacturing Innovation grant, MD Anderson Cancer Center via the Charles and Daneen Stiefel Center for Head and Neck Cancer Oropharyngeal Cancer Research Program and the MD Anderson Image Guided Cancer Therapy Research Program, Patient-Centered Outcomes Research Institute, Small Business Innovation Research Grant Program sub-award from Oncospace, and Elekta; royalties from Kallisio for licensed patent; honoraria and travel funds for attending meetings from Elekta, Philips Medical Systems, Varian/Siemens Healthineers, The American Association of Physicists in Medicine (AAPM), Massachusetts General Hospital, University of Alabama-Birmingham, Corewell Health System, Emory University, The American Society of Clinical Oncology (ASCO), The Royal Australian and New Zealand College of Radiologists, The American Society for Radiation Oncology (ASTRO), and The European Society for Radiotherapy and Oncology; committee member or study section service for NIH, AAPM, ASCO, ASTRO, Elekta, and MR-Linac Consortium; in-kind support from Elekta and Philips Medical Systems. **K.M.** No relevant relationships. **V.M.** No relevant relationships. **M.O.** Grant support from National Institute of Diabetes and Digestive and Kidney Diseases and NIBIB. **L.J.W.** No relevant relationships. **R.A.** No relevant relationships. **T.A.** No relevant relationships. **N.M.d.S.** Participant on a data safety monitoring board or advisory board for the European Institute for Biomedical Imaging Research; grant review panels for Cancer Research UK, Medical Research Council UK, and European Union Horizon Programme. **D.J.M.** No relevant relationships. **T.L.C.** Grants from the NIH; license for patent through the University of Michigan with Philips Healthcare and Siemens Healthineers; member of QIBA.

References

1. deSouza NM, Winfield JM, Waterton JC, et al. Implementing diffusion-weighted MRI for body imaging in prospective multicentre trials: current considerations and future perspectives. Eur Radiol 2018;28(3):1118–1131.
2. Gaur S, Harmon S, Rosenblum L, et al. Can apparent diffusion coefficient values assist PI-RADS Version 2 DWI scoring? A correlation study using the PI-RADSv2 and International Society of Urological Pathology systems. AJR Am J Roentgenol 2018;211(1):W33–W41.
3. Partridge SC, Zhang Z, Newitt DC, et al. Diffusion-weighted MRI findings predict pathologic response in neoadjuvant treatment of breast cancer: the ACRIN 6698 multicenter trial. Radiology 2018;289(3):618–627.
4. Labeur TA, Runge JH, Klompenhouwer EG, Klümpen HJ, Takkenberg RB, van Delden OM. Diffusion-weighted imaging of hepatocellular carcinoma before and after transarterial chemoembolization: role in survival prediction and response evaluation. Abdom Radiol (NY) 2019;44(8):2740–2750.
5. Huang MM, Macura KJ, Landis P, et al. Evaluation of apparent diffusion coefficient as a predictor of grade reclassification in men on active surveillance for prostate cancer. Urology 2020;138:84–90.
6. Ellingson BM, Gerstner ER, Smits M, et al. Diffusion MRI phenotypes predict overall survival benefit from anti-VEGF monotherapy in recurrent glioblastoma: converging evidence from phase II trials. Clin Cancer Res 2017;23(19):5745–5756.
7. Raunig DL, McShane LM, Pennello G, et al. Quantitative imaging biomarkers: a review of statistical methods for technical performance assessment. Stat Methods Med Res 2015;24(1):27–67.
8. Cashmore MT, McCann AJ, Wastling SJ, McGrath C, Thornton J, Hall MG. Clinical quantitative MRI and the need for metrology. Br J Radiol 2021;94(1120):20201215.
9. QIBA DWI Biomarker Committee. QIBA Profile: Magnetic Resonance Diffusion-Weighted Imaging (DWI) of the Apparent Diffusion Coefficient (ADC), Clinically Feasible Version. https://doi.org/10.1148/QIBA/20221215. Published December 15, 2022. Accessed August 2024.
10. Carr ME, Keenan KE, Rai R, et al. Conformance of a 3T radiotherapy MRI scanner to the QIBA Diffusion Profile. Med Phys 2022;49(7):4508–4517.
11. Shukla-Dave A, Obuchowski NA, Chenevert TL, et al. Quantitative Imaging Biomarkers Alliance (QIBA) recommendations for improved precision of DWI and DCE-MRI derived biomarkers in multicenter oncology trials. J Magn Reson Imaging 2019;49(7):e101–e121.
12. Malyarenko DI, Newitt D, Wilmes LJ, et al. Demonstration of nonlinearity bias in the measurement of the apparent diffusion coefficient in multicenter trials. Magn Reson Med 2016;75(3):1312–1323.
13. Palacios EM, Martin AJ, Boss MA, et al. Toward precision and reproducibility of diffusion tensor imaging: a multicenter diffusion phantom and traveling volunteer study. AJNR Am J Neuroradiol 2017;38(3):537–545.
14. Boss MA, Snyder BS, Kim E, et al. Repeatability and reproducibility assessment of the apparent diffusion coefficient in the prostate: a trial of the ECOG-ACRIN Research Group (ACRIN 6701). J Magn Reson Imaging 2022;56(3):668–679.
15. Newitt DC, Zhang Z, Gibbs JE, et al. Test-retest repeatability and reproducibility of ADC measures by breast DWI: results from the ACRIN 6698 trial. J Magn Reson Imaging 2018;49(6):1617–1628.
16. Newitt DC, Amouzandeh G, Partridge SC, et al. Repeatability and reproducibility of ADC histogram metrics from the ACRIN 6698 Breast Cancer Therapy Response Trial. Tomography 2020;6(2):177–185.
17. Obuchowski NA, Bullen J. Quantitative imaging biomarkers: effect of sample size and bias on confidence interval coverage. Stat Methods Med Res 2018;27(10):3139–3150.
18. Huang EP, Wang XF, Choudhury KR, et al. Meta-analysis of the technical performance of an imaging procedure: guidelines and statistical methodology. Stat Methods Med Res 2015;24(1):141–174.
19. Fedorov A, Vangel MG, Tempany CM, Fennessy FM. Multiparametric magnetic resonance imaging of the prostate: repeatability of volume and apparent diffusion coefficient quantification. Invest Radiol 2017;52(9):538–546.
20. Gibbs P, Pickles MD, Turnbull LW. Repeatability of echo-planar-based diffusion measurements of the human prostate at 3 T. Magn Reson Imaging 2007;25(10):1423–1429.
21. Litjens GJ, Hambrock T, Hulsbergen-van de Kaa C, Barentsz JO, Huisman HJ. Interpatient variation in normal peripheral zone apparent diffusion coefficient: effect on the prediction of prostate cancer aggressiveness. Radiology 2012;265(1):260–266.
22. Pfefferbaum A, Adalsteinsson E, Sullivan EV. Replicability of diffusion tensor imaging measurements of fractional anisotropy and trace in brain. J Magn Reson Imaging 2003;18(4):427–433.
23. Bonekamp D, Nagae LM, Degaonkar M, et al. Diffusion tensor imaging in children and adolescents: reproducibility, hemispheric, and age-related differences. Neuroimage 2007;34(2):733–742.
24. Paldino MJ, Barboriak D, Desjardins A, Friedman HS, Vredenburgh JJ. Repeatability of quantitative parameters derived from diffusion tensor imaging in patients with glioblastoma multiforme. J Magn Reson Imaging 2009;29(5):1199–1205.
25. Deckers F, De Foer B, Van Mieghem F, et al. Apparent diffusion coefficient measurements as very early predictive markers of response to chemotherapy in hepatic metastasis: a preliminary investigation of reproducibility and diagnostic value. J Magn Reson Imaging 2014;40(2):448–456.
26. Heijmen L, Ter Voert EE, Nagtegaal ID, et al. Diffusion-weighted MR imaging in liver metastases of colorectal cancer: reproducibility and biological validation. Eur Radiol 2013;23(3):748–756.
27. Miquel ME, Scott AD, Macdougall ND, Boubertakh R, Bharwani N, Rockall AG. In vitro and in vivo repeatability of abdominal diffusion-weighted MRI. Br J Radiol 2012;85(1019):1507–1512.
28. Zhang KS, Neelsen CJO, Wennmann M, et al. Same-day repeatability and between-sequence reproducibility of mean ADC in PI-RADS lesions. Eur J Radiol 2023;165:110898.
29. Rogers HJ, Singh S, Barnes A, et al. Test-retest repeatability of ADC in prostate using the multi *b*-value VERDICT acquisition. Eur J Radiol 2023;162:110782.
30. Barrett T, Lawrence EM, Priest AN, et al. Repeatability of diffusion-weighted MRI of the prostate using whole lesion ADC values, skew and histogram analysis. Eur J Radiol 2019;110:22–29.
31. Szasz T, Lee G, Chatterjee A, et al. Physically implausible signals as a quantitative quality assessment metric in prostate diffusion-weighted MR imaging. Abdom Radiol (NY) 2022;47(7):2500–2508.
32. Obuchowski NA. Interpreting change in quantitative imaging biomarkers. Acad Radiol 2018;25(3):372–379.
33. Hoang-Dinh A, Nguyen-Quang T, Bui-Van L, Gonindard-Melodelima C, Souchon R, Rouvière O. Reproducibility of apparent diffusion coefficient measurement in normal prostate peripheral zone at 1.5T MRI. Diagn Interv Imaging 2022;103(11):545–554.

34. Michoux NF, Ceranka JW, Vandemeulebroucke J, et al. Repeatability and reproducibility of ADC measurements: a prospective multicenter whole-body-MRI study. Eur Radiol 2021;31(7):4514–4527.
35. Jerome NP, Vidić I, Egnell L, et al. Understanding diffusion-weighted MRI analysis: repeatability and performance of diffusion models in a benign breast lesion cohort. NMR Biomed 2021;34(7):e4508.
36. Boss MA, Keenan KE, Stupic KF, et al. Magnetic Resonance Imaging Biomarker Calibration Service: NMR Measurement of Isotropic Water Diffusion Coefficient. https://nvlpubs.nist.gov/nistpubs/SpecialPublications/NIST.SP.250-100.pdf. Published March 2023. Accessed August 2024.
37. Amouzandeh G, Chenevert TL, Swanson SD, Ross BD, Malyarenko DI. Technical note: temperature and concentration dependence of water diffusion in polyvinylpyrrolidone solutions. Med Phys 2022;49(5):3325–3332.
38. Sorace AG, Wu C, Barnes SL, et al. Repeatability, reproducibility, and accuracy of quantitative mri of the breast in the community radiology setting. J Magn Reson Imaging 2018;48(3):695–707.
39. Hu Y, Hu Q, Zhan C, Yin T, Ai T. Intraobserver and interobserver reproducibility of breast diffusion-weighted imaging quantitative parameters: readout-segmented vs. single-shot echo-planar imaging. J Magn Reson Imaging 2023;58(6):1725–1736.
40. Ueno Y, Tamada T, Sofue K, et al. Do the variations in ROI placement technique have influence for prostate ADC measurements? Acta Radiol Open 2022;11(3):20584601221086500.
41. Spick C, Bickel H, Pinker K, et al. Diffusion-weighted MRI of breast lesions: a prospective clinical investigation of the quantitative imaging biomarker characteristics of reproducibility, repeatability, and diagnostic accuracy. NMR Biomed 2016;29(10):1445–1453.
42. deSouza NM, van der Lugt A, Deroose CM, et al. Standardised lesion segmentation for imaging biomarker quantitation: a consensus recommendation from ESR and EORTC. Insights Imaging 2022;13(1):159.
43. Paudyal R, Konar AS, Obuchowski NA, et al. Repeatability of quantitative diffusion-weighted imaging metrics in phantoms, head-and-neck and thyroid cancers: preliminary findings. Tomography 2019;5(1):15–25.
44. Lawrence LSP, Chan RW, Chen H, et al. Accuracy and precision of apparent diffusion coefficient measurements on a 1.5 T MR-Linac in central nervous system tumour patients. Radiother Oncol 2021;164:155–162.
45. van Pelt V, Navest RJM, Nowee ME, van der Heide UA, van Houdt PJ. Repeatability of free breathing diffusion weighted MRI for MR guided liver SBRT. Radiother Oncol 2021;161:S144–S145.
46. Habrich J, Boeke S, Nachbar M, et al. Repeatability of diffusion-weighted magnetic resonance imaging in head and neck cancer at a 1.5 T MR-Linac. Radiother Oncol 2022;174:141–148.
47. McDonald BA, Salzillo T, Mulder S, et al. Prospective evaluation of in vivo and phantom repeatability and reproducibility of diffusion-weighted MRI sequences on 1.5 T MRI-linear accelerator (MR-Linac) and MR simulator devices for head and neck cancers. Radiother Oncol 2023;185:109717.
48. Vergara D, Armato SG 3rd, Hadjiiski L, Drukker K. Best practices for artificial intelligence and machine learning for computer-aided diagnosis in medical imaging. J Am Coll Radiol 2024;21(2):341–343.
49. Lim CS, Abreu-Gomez J, Thornhill R, et al. Utility of machine learning of apparent diffusion coefficient (ADC) and T2-weighted (T2W) radiomic features in PI-RADS version 2.1 category 3 lesions to predict prostate cancer diagnosis. Abdom Radiol (NY) 2021;46(12):5647–5658.